

Alkaline pH Block of CLC-K Kidney Chloride Channels Mediated by a Pore Lysine Residue

Antonella Gradogna and Michael Pusch*

Istituto di Biofisica, Consiglio Nazionale delle Ricerche, Genoa, Italy

ABSTRACT CLC-K chloride channels are expressed in the kidney and the inner ear, where they are involved in NaCl reabsorption and endolymph production, respectively. These channels require the beta subunit barttin for proper function. Mutations in CIC-Kb and barttin, lead to Bartter's syndrome. Block of CLC-K channels by acid pH was described in a previous work, and we had identified His-497 as being responsible for the acidic block of CLC-K channels. Here, we show that CIC-K currents are blocked also by alkaline pH with an apparent pK value of ~ 8.7 for CIC-K1. Using noise analysis, we demonstrate that alkaline block is mediated by an allosteric reduction of the open probability. By an extensive mutagenic screen we identified K165, a highly conserved residue in the extracellular vestibule of the channel, as the major element responsible for the alkaline pH modulation. Deprotonation of K165 underlies the alkaline block. However, MTS modification of the K165C mutant demonstrated that not only the charge but also the chemical and sterical properties of lysine 165 are determinants of CLC-K gating.

INTRODUCTION

CLC-K channels belong to the family of CLC proteins comprising both Cl^- channels and Cl^-/H^+ antiporters. Members of this family are found in several tissues and organs where anion transport is important.

In humans, CLC-K channels comprise CIC-Ka and CIC-Kb (in rodents they are called CIC-K1 and CIC-K2). They were isolated from kidney by sequence homology with other CLC proteins (1,2). The human CLC-Ks have 90% identity to each other and 80% identity to rodent CLC-Ks (1). The combined action of the Na-K-ATPase, the apical $\text{Na}^+\text{-K}^+\text{-2Cl}^-$ cotransporter NKCC2, the apical K^+ channel ROMK, and the basolateral chloride channel CIC-Kb/barttin, leads to NaCl reabsorption in the thick ascending limb (TAL) of Henle's loop (3,4). CLC-Ks were identified also in the inner ear in the basolateral membrane of the marginal cells of the stria vascularis and in the dark cells of the vestibular organ (5). Both isoforms contribute to the maintenance of the high K^+ concentration and the positive potential of the endolymph (5–7). Both in the kidney and in the inner ear, CLC-Ks coassemble with the β -subunit, barttin, which affects the trafficking and the function of these channels (5,8–10). Mutations in the NKCC2 transporter, the ROMK channel, or the CIC-Kb channel cause different forms of the same renal disease, Bartter's syndrome, which demonstrates the common role of these proteins in NaCl reabsorption (11–13). Another form of Bartter's syndrome that includes deafness arises from mutations of barttin or from simultaneous mutations of CIC-Ka and CIC-Kb (8,14).

The regulation of CLC-K channels by various extracellular ligands has been the subject of several previous publications (15–22). External Ca^{2+} and protons have been found

to modulate these channels in the physiological concentration range (5,23–25). Currents are activated by extracellular Ca^{2+} , whereas high $[\text{H}^+]_{\text{ext}}$ (acidic pH) completely blocks CLC-Ks. Previously, a detailed biophysical analysis of the Ca^{2+} and proton effect on the human CIC-Ka showed that Ca^{2+} and protons affect the open probability of the channel via independent mechanisms and binding sites (25). An extensive mutagenic screen performed on CIC-Ka allowed us to identify four acidic residues, E259, E261, D278, and E281, that likely form an intersubunit Ca^{2+} -binding site (25,26). Modulation by protons is a characteristic found in most CLC proteins, both in Cl^-/H^+ antiporters and in CLC channels. Since protons are one of the substrates of the antiporters, it is not surprising that the Cl^-/H^+ exchange is influenced by varying the H^+ concentration (27–31). In most CLC channels, a highly conserved glutamate, the gating glutamate, has been found to be responsible for proton modulation (32–44). For example, in the CIC-0 channel, extracellular protons bind the gating glutamate and increase the open probability (36,38). Interestingly, intracellular acidic pH also activates CIC-0. Intracellular protons binding to the same glutamate lead to a shift of the voltage dependence of the open probability to more negative voltages (32,40–42). The effect of external protons on the gating is seen at acidic pH, whereas CIC-0 currents do not change from neutral to alkaline conditions (36). The gating of the CIC-1 channel, similar to that of CIC-0, is affected both by external and internal pH (33,45). Interestingly, the pH regulation of the CIC-2 channel is quite different from that of CIC-0. First, intracellular pH has only small effects on the open probability (44), but the channel shows a biphasic response to extracellular pH, with block both at alkalization and at acidification (34,37,39,43,44). Activation and inhibition arise from the protonation of two different residues: the protonation of the gating glutamate

Submitted February 13, 2013, and accepted for publication May 24, 2013.

*Correspondence: pusch@ge.ibf.cnr.it

Editor: William Kobertz.

© 2013 by the Biophysical Society
0006-3495/13/07/0080/11 \$2.00

<http://dx.doi.org/10.1016/j.bpj.2013.05.044>



activates the channel (39), whereas the protonation of an off-pore extracellular histidine inactivates the channel (43).

Similar to the case for CLC-2, CLC-K channels are also blocked by acidic pH (5,24,25,46), and in fact, they share the histidine residue (H497, corresponding to H532 of CLC-2), which was found to be responsible for H⁺-induced block of CLC-Ka (25). In contrast, CLC-K channels lack the gating glutamate, whose deprotonation underlies the inactivation of CLC-2 currents at alkaline pH. Here, we found that despite this, CLC-K channels are strongly blocked by alkaline pH via a reduction of the open probability. By an extensive mutagenic screen and cysteine modifications, we identified a pore lysine, K165, whose deprotonation likely mediates this block.

MATERIALS AND METHODS

Molecular biology

Mutants of CLC-Ka and CLC-K1 were obtained by recombinant PCR as described previously (47). All new constructs were sequenced and coexpressed with the barttin mutant Y98A (5). The cRNA of CLC-K constructs was prepared using the AmpliCAP SP6 Message Maker kit (Biospa, Italy) after linearization with MluI, whereas the cRNA of Y98 barttin was transcribed by the mMessage mMachine T7 kit (Life Technologies, Italy) after linearization with NotI. All wild-type (WT) cDNA constructs were kindly provided by T. J. Jentsch.

Electrophysiology

The cRNA of CLC-K and barttin constructs was coinjected in defolliculated *Xenopus* oocytes, which were incubated at 18°C in the maintaining solution containing (in mM) 90 NaCl, 2 KCl, 1 MgCl₂, 1 CaCl₂, and 10 Hepes (pH 7.5). One to five days after the injection, voltage-clamp measurements were performed at room temperature using the custom acquisition program GePulse (available at <http://users.ge.ibf.cnr.it/pusch/programs-mik.htm>) and a Turbo TEC-03X amplifier (npi electronics, Tamm, Germany). The standard bath solution contained (in mM) 112 NaCl, 10 Ca-Gluconate₂, 1 MgSO₄, and 10 HEPES (pH 7.3) (osmolality, 227 mOsm). HEPES was replaced by MES buffer in solutions at pH <7, Bis-tris propane in solutions at pH 9, and CAPS in solutions at pH >9.

The membrane was kept at a holding potential corresponding to the resting membrane potential (−30 mV). To evaluate CLC-K currents at different voltages, a stimulation protocol was applied as follows (IV-pulse protocol). A prepulse to −100 mV for 100 ms was followed by voltages ranging from −140 to 80 mV with 20-mV increments for 200 ms. Pulses ended with a tail to 60 mV for 100 ms. The effect of the different pH values was monitored by applying 200-ms pulses to 60 mV once per second. The records were taken under continuous perfusion with the desired solution until steady state was reached. The stability of the currents was verified by applying the standard bath solution at the end of the experiment, while endogenous currents were estimated by using a solution containing (in mM) 100 NaI, 5 MgSO₄, and 10 Hepes (pH 7.3) that inhibits only CLC-K channels (20). The effect of pH was quantified by the ratio of the current measured at a specific pH to that in standard bath solution. Leak currents (i.e., residual currents in iodide) were subtracted.

Modification of K165C CLC-K1 by methanethiosulfonate reagents

Methanethiosulfonate (MTS) reagents (Biotium, Hayward, CA) and dithiothreitol (DTT) were dissolved in the standard bath solution immediately

before use and kept on ice during the experiments. For 2-hydroxyethyl methanethiosulfonate (MTSEH), a 1 M stock solution was prepared in dimethyl sulfoxide (DMSO) and stored at −80°C. A typical experiment involving MTS modification was performed in several stages. Before modification, CLC-K1 K165C currents were measured at various pH values (from 7.3 to 11). Then the oocyte was removed from the set-up and incubated in a solution containing 1 mM MTS reagent. Incubation time was 10 min for 2-aminoethyl methanethiosulfonate (MTSEA), 15 min for MTSEH, and 60 min for 2-(trimethylammonium) ethyl methanethiosulfonate (MTSET). Finally, the oocyte was placed back in the recording chamber and currents were measured at various pH values. For experiments with MTSEA and MTSEH, the recordings ended with the perfusion of 10 mM DTT, followed by a washout using the standard solution. For experiments with MTSET, which did not induce a change of currents, modification efficiency was verified by an additional treatment with 1 mM MTSEA.

The experiments to determine the reaction rate of K165C CLC-K1 with MTSEA or MTSEH were performed under continuous perfusion of 1 mM MTSEA or MTSEH. The current was monitored by repetitive 200-ms pulses to 60 mV once per second. The speed of perfusion was estimated by the speed of iodide block and found to be faster than ~2 s, significantly faster than the speed of modification by MTS reagents at 1 mM.

MTS modification was quantified as the ratio of the current measured in standard bath solution after MTS treatment to that measured before incubation. Leak currents were subtracted.

Noise analysis

Patch-clamp measurements were performed in the inside-out configuration. The intracellular (bath) solution contained (in mM) 100 *N*-methyl-D-glucamine-Cl (NMDG-Cl), 2 MgCl₂, 1 EGTA, and 10 HEPES (pH 7.3). An intracellular solution in which Cl[−] was replaced by glutamate was used to evaluate endogenous and leak currents. The extracellular solution contained (in mM) 92 tetraethylammonium chloride (TEA-Cl), 10 CaCl₂, and 10 HEPES (pH 7.3) or, alternatively, 92 TEA-Cl, 10 CaCl₂, and 10 CAPS (pH 10). Pipettes were pulled from borosilicate glass capillaries (Hilgenberg, Malsfeld, Germany) and had resistances of 1–2 MΩ in the recording solutions. To estimate the single-channel current by noise analysis, the following stimulation protocol was applied 50–100 times: a prepulse to 60 mV was followed by a pulse to −100 mV for 500 ms. Pulses ended with a tail at 60 mV for 200 ms. Currents were recorded at 50 kHz after filtering at 10 kHz with an eight-pole Bessel filter. Data analysis was performed at two potentials, −100 mV and +60 mV. The mean current, I , was first calculated. The variance, σ^2 , was estimated from the averaged squared difference of consecutive traces with the background variance at 0 mV subtracted. The variance-mean plot was assembled by binning as described previously (48). Finally the variance-mean plot was fitted by $\sigma^2 = iI - I^2/N$, with the single-channel current, i , and the number of channels, N , as free parameters (49).

RESULTS AND DISCUSSION

Alkaline pH blocks CLC-K channels

In our previous work (25), we examined how high [H⁺]_{ext} affects CLC-K channels, and found that the protonation of an extracellularly facing histidine, H497, is responsible for the block of CLC-K-mediated currents at acidic pH (25). Here, we investigated the effect of alkalization on the currents of human CLC-Ka and CLC-Kb and of rodent CLC-K1, extending the pH range examined to include values from pH 5 to pH 11. Interestingly, alkaline pH blocks all CLC-K channels, with remaining currents at pH 11 being <~6%

of the currents recorded in control conditions (pH 7.3, 10 mM Ca^{2+}) for CIC-Ka and CIC-K1 (Fig. 1 A), and with a strong block of CIC-Kb also (Fig. S1 A in the Supporting Material). The observation that CIC-Ka, CIC-Kb, and CIC-K1 show the highest current levels at different pH values (Fig. 1 A and Fig. S1 A) could be due to different degrees of block by acidic pH, alkaline pH, or both. The lines in Fig. 1 A are derived from a quantitative model discussed below.

The drastic block by alkaline pH is further highlighted by the current traces evoked by the IV-pulse protocol (see Materials and Methods) at different pH values from oocytes expressing CIC-Ka (Fig. 1 B), CIC-K1 (Fig. 1 C), or CIC-Kb (Fig. S1 B). These data show that low $[\text{H}^+]_{\text{ext}}$ reduces the current density without dramatically modifying the kinetics of the currents.

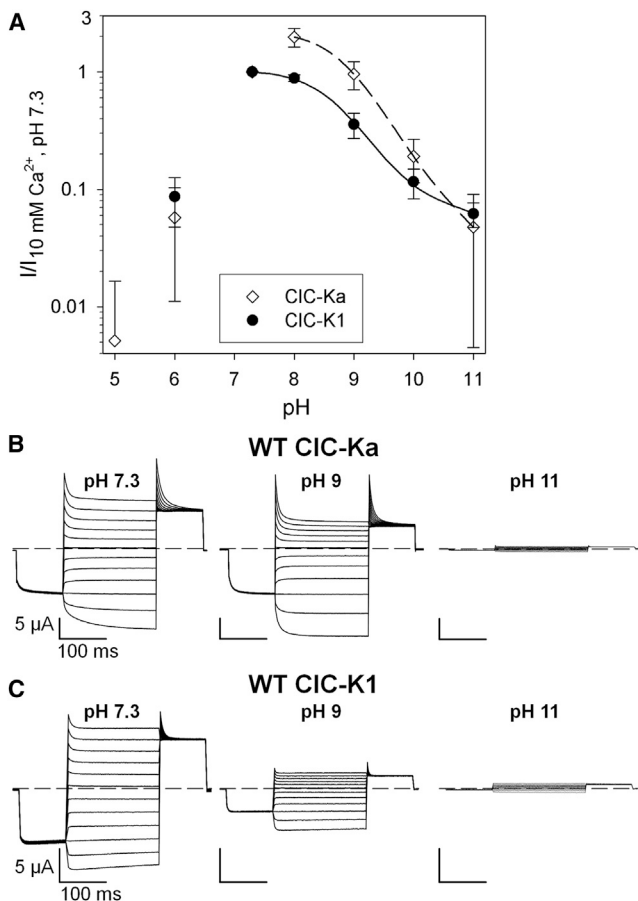


FIGURE 1 Effect of alkaline pH on WT CIC-Ka and WT CIC-K1. (A) Mean currents of CIC-Ka ($n \geq 11$; solid circles) and CIC-K1 (open diamonds; $n \geq 7$) at 60 mV recorded at pH values between 5 and 11 were normalized to the current measured in standard bath solution and plotted versus pH. The lines represent the best fit of WT CIC-Ka currents (dashed line; fit parameters, $\text{pK} = 8.9$, $\text{pL} = 11.3$, and $R = 0.02$) and WT CIC-K1 (solid line; fit parameters, $\text{pK} = 8.7$, $\text{pL} = 11.8$, and $R = 0.07$) obtained by Eq. 1, as described in Results. Error bars indicate the SD. (B and C) Typical current traces of WT CIC-Ka (B) and WT CIC-K1 (C) evoked by the IV-pulse protocol (see Materials and Methods) at pH 7.3, 9, and 11.

An important question is whether alkaline pH has a direct effect on the ion permeation or whether it acts indirectly by modulating the open probability. Because preliminary single-channel recordings performed on WT CIC-K1 at pH 7.3 had a very flickery behavior (data not shown), we estimated the single-channel conductance at neutral and alkaline pH using nonstationary noise analysis. This approach also allowed us to discriminate small changes of current by varying external pH. These inside-out patch-clamp experiments were performed on CIC-K1 because of its higher functional expression compared to human CLCs. Using extracellular (pipette) solutions at pH 7.3 or pH 10, repetitive pulses to 60 mV were applied after a prepulse to -100 mV. Mean current and variance were evaluated (Fig. 2, A and B, left), and the single-channel current

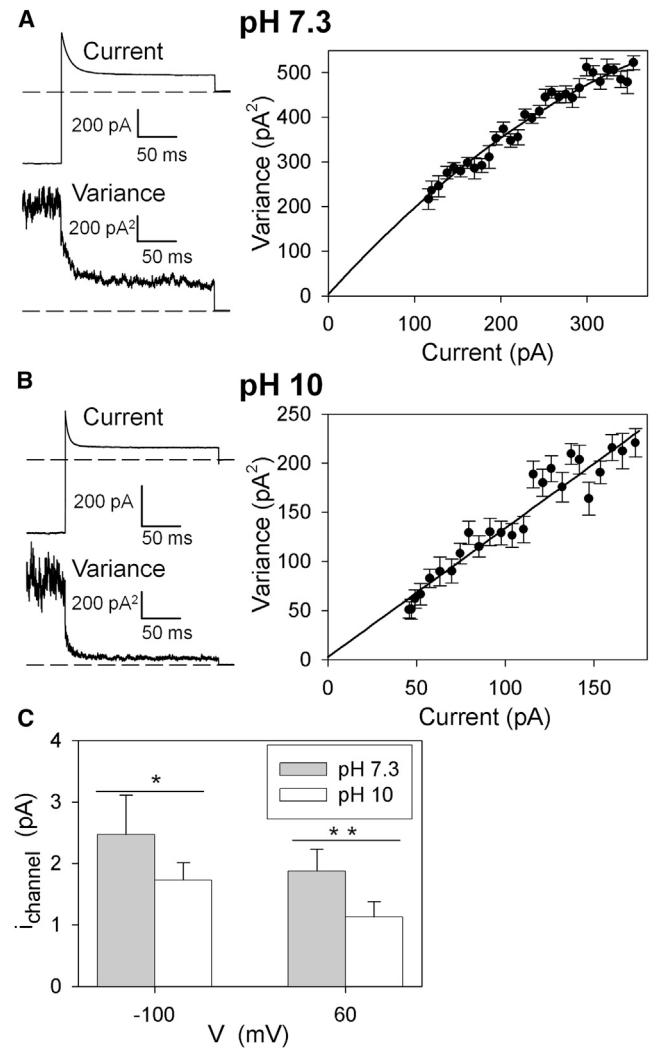


FIGURE 2 (A and B) Nonstationary noise analysis of WT CIC-K1 at pH 7.3 (A) and pH 10 (B). (Left) Mean current (upper) and variance (lower) are shown as a function of time. (Right) Variance (symbols) is plotted versus the mean current and fitted with a parabola (line), as described in Materials and Methods. (C) Bars represent the mean single-channel current at different pH values and potentials. * $P < 0.05$; ** $P < 0.005$ (unpaired Student's t -test). Error bars indicate the SD.

was estimated by the best fit of a parabola to the variance as a function of the mean current (Fig. 2, A and B, right), as described in Materials and Methods. The data cover only the initial linear part of the parabola due to the small open probability. Nevertheless, the fit provides a robust estimate of the single-channel current. Results are summarized in Fig. 2 C: in depolarizing conditions (+60 mV), the single-channel current at pH 10 is ~60% of the current at pH 7.3; similarly, at -100 mV, the current is ~70% of that at pH 7.3. This relatively small reduction of the conductance at pH 10 is not able to explain the reduction of macroscopic currents (at pH 10, CIC-K1 currents are ~12% of those at pH 7.3). Thus, we conclude that alkaline pH acts mainly by an allosteric reduction of the open probability.

Scanning mutagenesis identifies a pore lysine as the most likely candidate to mediate the effect of alkaline pH

Since histidine 497, responsible for the acidic block of CLC-K currents (25), is not involved in the alkaline inhibition of these channels (data not shown), other residue(s) had to be implicated in this process. To identify these residues, we used the same strategy employed successfully in our previous work (25): based on the crystal structure of the homologous bacterial EcCIC (38,50), we chose and mutated all titratable residues of CIC-Ka for which deprotonation at alkaline pH is plausible (C, H, K, R, and Y) and which are accessible from the extracellular side of the pore (Fig. 3 A). In general, the mutations inserted neutralized charged residues and/or replaced titratable with nontitratable residues. The 29 selected residues are colored in pink and light blue in the surface representation of the two subunits of a homology model of CIC-Ka (26) (Fig. 3). All constructs were coexpressed with barttin in *Xenopus* oocytes and tested for their response to alkaline pH. Alkaline pH inhibited all CIC-Ka mutants tested, but few of them showed a weakened sensitivity (Fig. 4, A–C). Our focus was on mutants in which a titratable residue was replaced by a nontitratable residue and whose response to alkaline pH was strongly modified. In case such mutants did not express, we also considered mutants in which a titratable residue was exchanged with another titratable amino acid and which exhibited a slight alteration of the pH dependence. Based on these criteria, the mutants chosen were K355A, Y520A, K268Q, and K165R. These mutants were examined in further detail, and when the data were not conclusive because of low current expression, the mutations were inserted in the background of CIC-K1, which shows larger expression than CIC-Ka. The pH sensitivity of K355A seems to be shifted, given that the currents recorded at pH 8 and 9 are fourfold larger than those at pH 7.3 (Fig. 4 B), which renders unlikely a direct involvement of K355 in alkaline block. Since also niflumic acid (at 200 μ M) is more effective on K355A than on WT, with a twofold larger

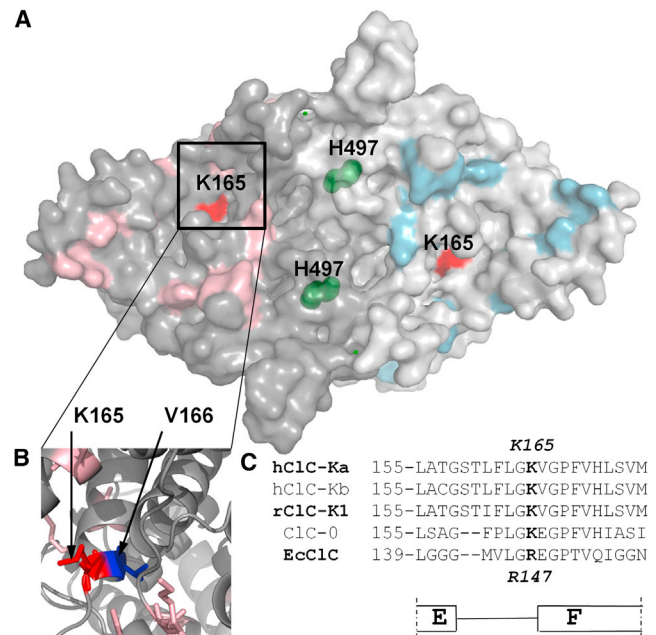


FIGURE 3 Mapping the mutants on the homology model of CIC-Ka. (A) Surface representation of the CIC-Ka model (26) based on the bacterial EcCIC homodimer (Protein Data Bank accession no. 1KPK (50)) viewed from the extracellular side. The two subunits are colored gray and light gray. The residues of CIC-Ka selected for mutation are shown in pink and light blue in the two subunits. The two residues that are involved in CLC-K modulation by pH, H497 and K165, are colored in green and red, respectively. Several residues of CIC-Ka (K355, R351, H357, H365, and H386) are not included in the homology model, because they are contained in portions of the channel that are not present in EcCIC. (B) Enlargement of the region containing K165 is shown in cartoon representation. K165 (R147 in EcCIC) and the neighboring V166 (E148 in EcCIC) are represented as sticks and colored in red and blue, respectively. (C) Alignment of sequences around K165.

potentiation compared to WT (see Fig. 3 of Zifarelli et al. (21)), it seems that mutating K355 to alanine renders CIC-Ka more sensitive to potentiation factors, suggesting that the mutant somehow alters the gating properties of the channel. Y520A CIC-Ka (Figs. 4 C and S2) is only slightly affected at pH 10, but is blocked at pH 11. Y520 corresponds to Y512 of CIC-0 and Y445 of EcCIC, a residue that is accessible to the intracellular solution and is involved in the coordination of pore chloride ions in the bacterial CLC homolog (47,50–52). In CIC-Ka and in CIC-K1 (data not shown), the mutant induces the appearance of very large currents that lack typical WT kinetics (Fig. S2 B). Thus, the relative insensitivity up to pH 10 likely reflects an indirect, unspecific effect of the mutant on gating. This phenotype, combined with the exposition of the residue to the intracellular (but not extracellular) solution, safely excludes deprotonation of Y520 as the process underlying the effects of alkaline external pH. The small currents of K268Q CIC-Ka made the effect of alkaline pH very difficult to evaluate properly (Fig. 4 B). However, in the context of CIC-K1, currents of mutant K268Q were similar to the WT in magnitude

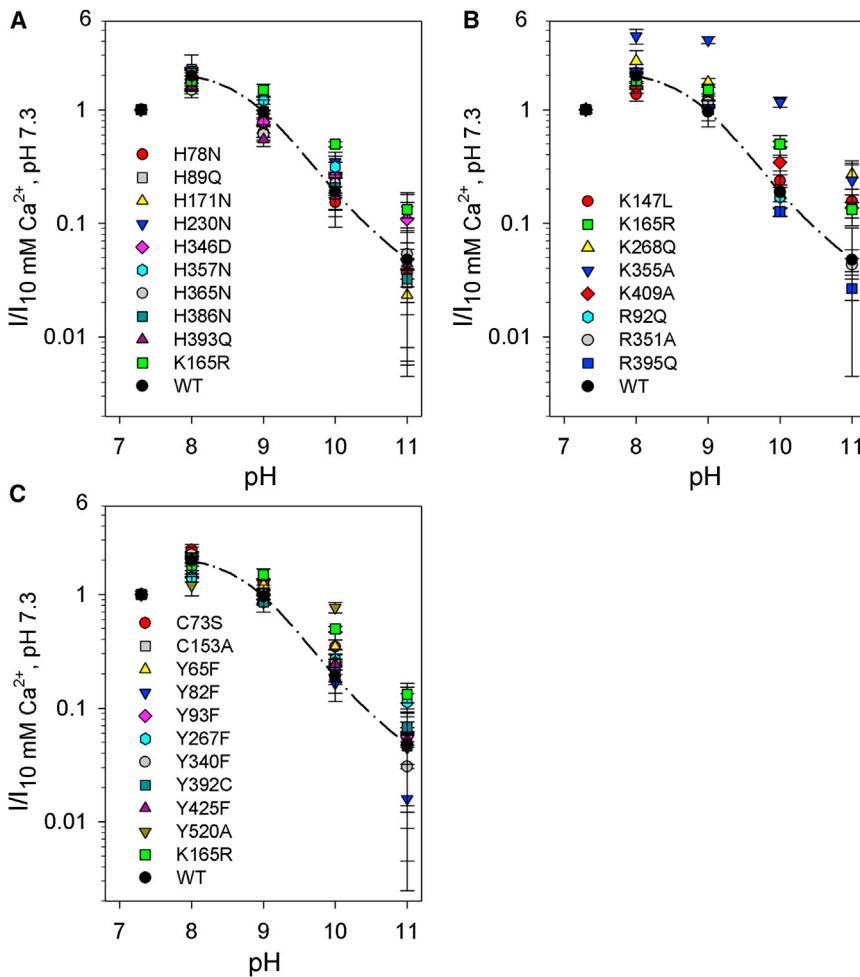


FIGURE 4 Effect of alkaline pH on all CIC-Ka mutants. To facilitate the data representation, the mutants were grouped by chemical properties of the mutated residues. The diagrams collect the data resulting from the mutations of histidine (A), lysine and arginine (B), and cysteine and tyrosine (C). The currents acquired at 60 mV were normalized to those measured at pH 7.3 ($n \geq 3$). Mutants R184G and H480N did not yield functional expression. Data and fit for WT CIC-Ka are the same as in Fig. 1 A. Data for K165R CIC-Ka are shown in all three groupings. Some variability in the response to alkaline pH is caused by different levels of functional expression of the mutants. Error bars indicate the SD.

and pH sensitivity (Fig. S3, A and B), excluding this residue also as responsible for mediating the block at alkaline pH.

K165, the only other residue from our experimental data (Fig. 4 B and Fig. S4) that emerged as possibly responsible for the channel's sensitivity to alkaline pH, is highly conserved in CLC proteins (53). This lysine is located in the E-F loop in the extracellular pore vestibule of the channel, next to V166, the residue corresponding to the gating glutamate that is shared by all CLC proteins except CLC-K channels (Fig. 3, A–C). The effect of alkaline pH on the K165R mutant is weakened compared to the WT (Fig. S4, A and B). The slight impairment is caused by the conservative mutation of lysine to arginine, which does not prevent deprotonation at this site. A stronger effect could be expected by substituting a nontitratable residue for K165. Unfortunately, the other mutations inserted in this position of CIC-Ka (K165A, K165C, K165H, and K165Q) did not show functional expression.

The lysine of CIC-1 and CIC-0 that corresponds to K165 of CIC-Ka has been the subject of previous studies (54,55). Lin and Chen (55) found that the nonfunctional K165C/C212S CIC-0 channel could be activated by reaction with

MTSEA, which confers a positive charge and changes the side chain of the cysteine to one that is lysine-like. The other MTS reagents tested, MTSET and 2-sulphonoethyl MTS (MTSES), did not induce currents (55). Since CIC-0 is ~39% identical to CIC-K channels (2), we hypothesized that the MTSEA reagent could also reactivate the dormant K165C CIC-Ka. Before testing this idea, we verified that MTSEA does not affect WT CIC-Ka currents by interacting with native cysteine residues (data not shown). When we applied MTSEA to K165C CIC-Ka-expressing oocytes, however, the currents elicited were too small to allow an easily quantitative investigation (data not shown). Also, as found for CIC-0, K165C CIC-Ka was not activated by the positively charged MTSET and the negatively charged MTSES (data not shown).

MTS-modified K165C CIC-K1 confirms the involvement of K165 in CLC-K modulation by alkaline pH

To obtain measurable currents from a nonconservative mutant of the K165 residue, we tried to insert the mutation

K165C in the background of the rat WT CIC-K1 channel, which has higher functional expression than WT CIC-Ka. Fortunately, the mutant K165C CIC-K1 channel shows functional expression even without activation by MTSEA. The currents are much smaller than those of WT CIC-K1 (Fig. 1 C), and the typical current kinetics of the channel are almost absent at pH 7.3 and just perceptible at pH 8 and 9 (Fig. 5 A). It is important to note that K165C CIC-K1 shows a modified sensitivity to alkaline pH compared to WT. For WT CIC-K1, maximal currents are measured at pH 7.3, and at pH 9, for example, they are only ~36% of those in control conditions (Fig. 5 B). Instead, for K165C, currents peak at pH 9, where they are more than twofold larger than those at pH 7.3. The current at pH 11 is comparable to that at pH 7.3 (Fig. 5, A and B), strongly suggesting that K165 is indeed involved in alkaline pH block (the lines in Fig. 5 B were derived from a quantitative model, discussed below). To investigate in more detail the pH sensitivity of K165C CIC-K1, we used the MTS reagents on this mutant. The MTS modification allowed us to obtain higher functional expression of the mutant and enabled us to study the effect of varying the charge and the titratability of the side chain at position 165. We used the positive, titrat-

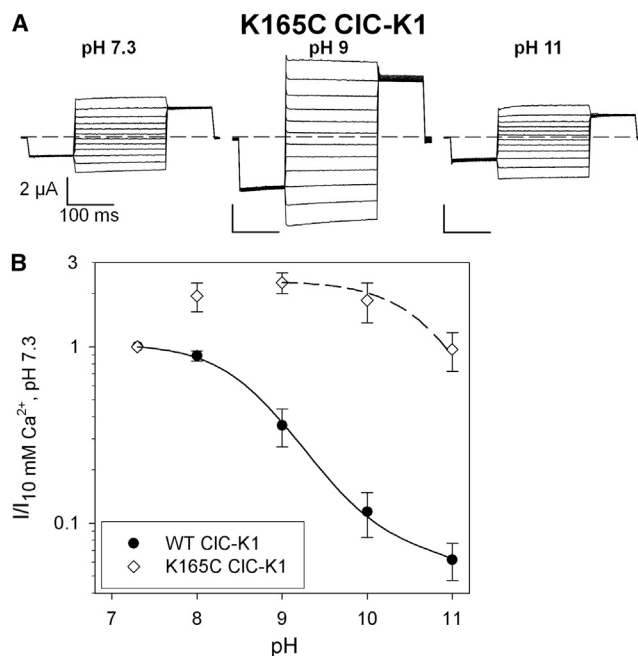


FIGURE 5 K165C CIC-K1 shows reduced sensitivity to alkaline pH. (A) Voltage-clamp traces in response to the IV-pulse protocol (see Materials and Methods) from the same oocyte under three different pH conditions. The small currents of K165C recorded before MTSEA activation were obtained by injecting ~2.5 ng of cRNA, whereas only ~0.1 ng of WT CIC-K1 cRNA was injected. (B) Effect of $[\text{H}^+]_{\text{ext}}$ on WT CIC-K1 (solid circles; $n = 10$) and K165C CIC-K1 (open diamonds; $n \geq 23$). Currents at 60 mV were normalized to the value recorded in standard bath solution (pH 7.3) and plotted versus pH. The dashed line represents the best fit of Eq. 2 to the K165C CIC-K1 currents ($pL = 10.8$). Data and fit for WT CIC-K1 are the same as in Fig. 1 A. Error bars indicate the SD.

able MTSEA, the neutral MTSEH, and the positive, nontitratable MTSET. None of these reagents had an effect on WT CIC-K1 currents (data not shown).

Because MTSEA and MTSEH modification cause an increase of the currents mediated by K165C CIC-K1, we could directly follow their modification of C165 (Fig. S5). MTSET was excluded from these measurements, because MTSET modification of K165C CIC-K1 was not accompanied by a change of the current level. From such experiments, in which the MTS reagent was continuously applied, we could estimate the time constant, τ , of modification (Fig. S5). From τ , we calculated the reaction rate, k , as $k = \tau^{-1}/1 \text{ mM}$. For MTSEA, we obtained $\tau = (4.9 \pm 1.0) \text{ s}$ and $k = (206 \pm 40) \text{ s}^{-1} \text{ M}^{-1}$ and for MTSEH, $\tau = (8.9 \pm 1.8) \text{ s}$ and $k = (112 \pm 23) \text{ s}^{-1} \text{ M}^{-1}$ (all errors are expressed as the mean \pm SD). These parameters provide a hint of the external accessibility of a residue. The reaction rate of K165C CLC-K1 with MTSEA is smaller than that found by Lin and Chen (55) for the analogous mutation K165C in CIC-0 ($4.6 \times 10^3 \text{ s}^{-1} \text{ M}^{-1}$), indicating that this residue is less accessible from the extracellular side in CIC-K1 than in CIC-0.

MTSEA treatment increases currents approximately fivefold (Fig. 6, A and B). Moreover, the MTSEA-modified K165C CIC-K1 partially recovers the time-dependent relaxations that characterize WT CIC-K1 (Fig. 6 A, right). It is interesting that the pH sensitivity of the MTSEA-modified mutant is different from that of both the unmodified K165C and the WT (Fig. 6 C). Slight alkalization beyond pH 7.3 reduces currents to a relative level of ~0.5 compared to the currents at pH 7.3, with a further reduction at pH 11. This phenotype indicates the presence of two distinct pH-dependent processes, which will be described in a quantitative model below. The strong qualitative effect of MTSEA modification on the pH dependence of K165C strengthens the conclusion that K165 is involved in at least one of these processes. MTSEA modification was reversible upon addition of 10 mM DTT: after perfusion with DTT, the current amplitude was restored to the phenotype before MTSEA treatment (Fig. 6 B). MTSEA converts C165 to a lysinlike residue with respect to charge and pK.

We next tested the neutral MTSEH. As for MTSEA, MTSEH modification increases current levels of K165C approximately threefold (Fig. 7, A and B). This indicates that the open probability is determined not only by the charge at position 165, but also by the general chemical and steric properties of the residue at this position. It is important to note that the sensitivity to alkaline pH is strongly reduced compared to that of WT CIC-K1 (Fig. 7 C), displaying a reduction of currents only at values beyond pH 10. The insensitivity of the MTSEH-modified K165C mutant at pH values ≤ 10 is again consistent with the idea that deprotonation of residue K165 underlies the major part of the alkaline pH dependence of CLC-K channels. Since MTSEH is not titratable, the reduction at pH 11 likely

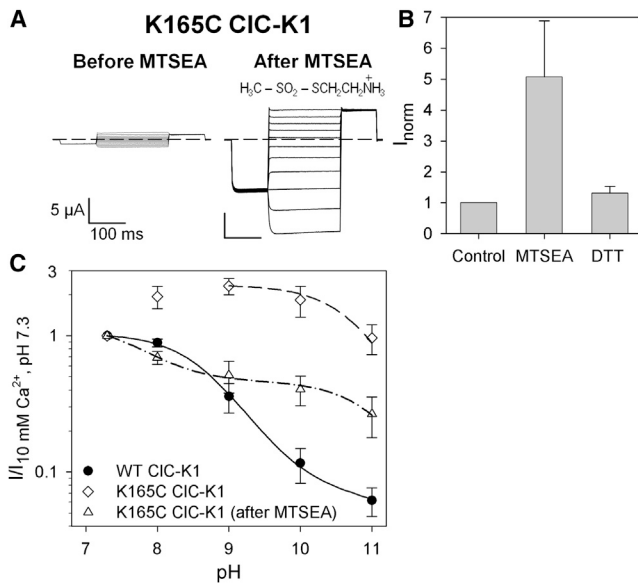


FIGURE 6 MTSEA-modified K165C CIC-K1 partially recovers the WT sensitivity to alkaline pH. (A) Current traces of K165C CIC-K1 evoked by the IV-pulse protocol (see Materials and Methods) from the same oocyte. The currents were recorded in the standard bath solution before (left) and after (right) incubation in 1 mM MTSEA. The chemical formula of MTSEA is shown. (B) Bars represent the normalized currents in standard bath solution under three different conditions: before MTSEA treatment (control), after incubation in 1 mM MTSEA ($n = 6$), and after a subsequent wash in 10 mM DTT ($n = 3$). Currents were normalized versus the current recorded at pH 7.3 before incubation in MTSEA. Error bars indicate the SD. (C) Mean currents at 60 mV from WT CIC-K1 (solid circles; $n = 10$), untreated K165C CIC-K1 (open diamonds; $n \geq 23$), and K165C CIC-K1 after incubation in 1 mM MTSEA (open triangles; $n \geq 5$) were normalized to the current at pH 7.3. The dot-dashed line represents the best fit of MTSEA-modified K165C currents obtained by Eq. 1, as described in Results. The fit parameters are $pK = 7.6$, $pL = 11.1$, and $R = 0.37$. Data and fit for WT CIC-K1 are the same as in Figs. 1 A and 5 B, those for K165C CIC-K1 are the same as in Fig. 5 B. Error bars indicate the SD.

reflects an additional process of deprotonation, unrelated to K165. DTT only partially reversed the MTSEH modification (Fig. 7 B).

Finally, we examined the effect of the positive and nontitratable MTSET reagent. MTSET treatment did not induce an increase in the current amplitude, raising the possibility that it does not react. To test this, we applied MTSEA after incubation with MTSET. Our expectation was that if MTSET did not react with C165, MTSEA treatment would increase currents about fivefold. Instead, MTSEA increased the current only ~1.6-fold, proving that most channels had reacted with MTSET (Fig. 8 A). The fact that modification by a positively charged reagent has, in the case of MTSET, no effect on the current level shows again that a charge at position 165 is not the only important parameter in determining open probability. The pH dependence of MTSET-modified K165C is very similar to that found after modification with MTSEH: currents are barely affected by pH values between 7.3 and 10, and at pH 11, MTSET-modi-

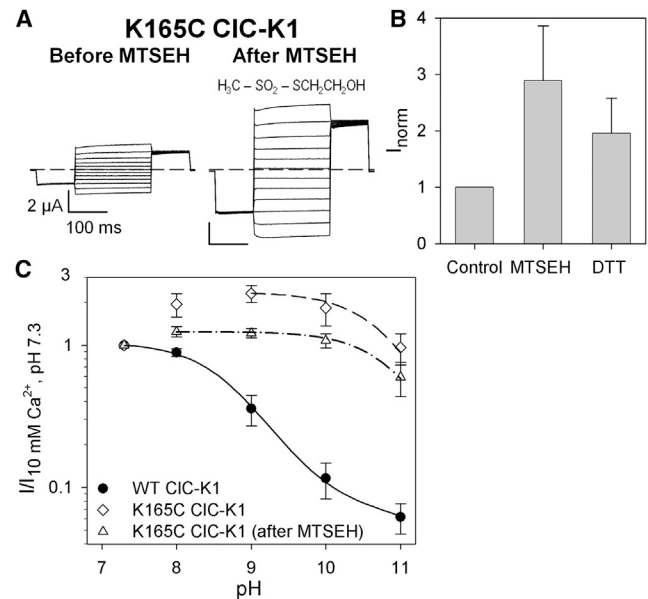


FIGURE 7 MTSEH-modified K165C CIC-K1 loses most of its sensitivity to alkaline pH. (A) Current responses to the IV-pulse protocol from an oocyte expressing K165C CIC-K1 before (left) and after (right) incubation in 1 mM MTSEH. The chemical formula of MTSEH is shown. (B) Mean values of currents before MTSEH treatment (Control), after incubation in 1 mM MTSEH ($n = 16$), and after a subsequent wash in 10 mM DTT ($n = 10$) were normalized to those recorded in standard bath solution before MTSEH perfusion. Error bars indicate the SD. (C) Mean currents measured at 60 mV at pH values ranging from 7.3 to 11 from WT CIC-K1 (solid circles; $n = 10$), untreated K165C CIC-K1 (open diamonds; $n \geq 23$), and K165C CIC-K1 after incubation in 1 mM MTSEH (open triangles; $n \geq 15$, except at pH 10, where $n = 8$) normalized to the current at pH 7.3. The dot-dashed line represents the best fit of Eq. 2 to the MTSEH-modified K165C currents with $pL = 10.9$. Data and fit for WT CIC-K1 are the same as in Figs. 1 A, 5 B, and 6 C; those for K165C CIC-K1 are the same as in Figs. 5 B and 6 C. Error bars indicate the SD.

fied K165C currents are ~59% of those at pH 7.3 (Fig. 8 B). However, keeping in mind that the MTSET-modified K165C has a low level of current, these data have to be considered cautiously. Nevertheless, we can conclude that without the titratability of K165, the channel loses most of its sensitivity to alkaline pH.

Modeling alkaline pH modulation of CLC-K channels

The mutagenesis of residue K165 and the various MTS modifications of K165C clearly establish that deprotonation of K165 underlies the reduction in open probability at pH values ≤ 10 . However, an additional pH-dependent process is revealed by the behavior of mutant K165C and by recordings of the mutant modified by nontitratable MTS reagents: at pH values > 10 , currents decrease in all circumstances.

To test these hypotheses in a quantitative manner, we invoke the simplest model incorporating these two pH-dependent processes: protonation/deprotonation of K165

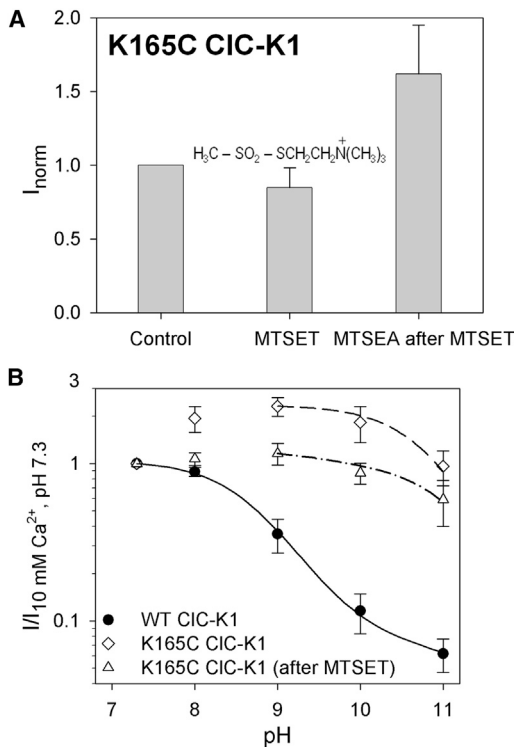
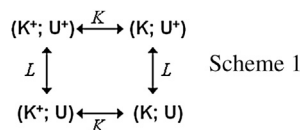


FIGURE 8 MTSET does not increase K165C current levels but strongly decreases sensitivity to alkaline pH. (A) Normalized current amplitudes in standard solution before modification by MTSET (*Control*), after incubation in 1 mM MTSET ($n = 8$), and after a subsequent treatment in 1 mM MTSEA ($n = 3$). Currents are normalized to those recorded in control conditions before treatment with MTS reagents. The chemical formula of MTSET is shown in the middle of the diagram. Error bars indicate the SD. (B) Voltage-clamp measurements at 60 mV of WT CIC-K1 (*solid circles*; $n = 10$), untreated K165C CIC-K1 (*open diamonds*; $n \geq 23$), and K165C CIC-K1 after incubation in 1 mM MTSET (*open triangles*; $n = 8$) were normalized to the current in standard bath solution and plotted versus pH. The dot-dashed line represents the best fit of Eq. 2 to the MTSET-modified K165C currents with $pL = 11.1$. Data and fit for WT CIC-K1 are the same as in Figs. 1 A, 5 B, 6 C, and 7 C; those for K165C CIC-K1 are the same as in Figs. 5 B, 6 C, and 7 C. Error bars indicate the SD.

(site K in Scheme 1), and protonation/deprotonation of an unknown site, U.



The model is composed of four states, as shown in Scheme 1. Deprotonation of site K and deprotonation of the unknown site are considered as independent processes governed by the dissociation constants K and L , respectively.

Protonated and deprotonated states of site K are associated with open probabilities P^+ and P^0 , respectively (states $(\text{K}^+; \text{U}^+)$ and $(\text{K}; \text{U}^+)$), whereas deprotonation of site U is

hypothesized to shut the channel completely. The latter assumption is difficult to test, because it would require exploration of pH values >11 . However, it is also of little relevance for the pH range considered here.

With these assumptions, for Scheme 1, the open probability is given by the equation

$$P = \frac{1}{\left(1 + \frac{L}{[\text{H}]}\right)} \left(\frac{P^+ \frac{[\text{H}]}{K} + P^0}{1 + \frac{[\text{H}]}{K}} \right), \quad (1)$$

where $[\text{H}]$ is the extracellular proton concentration. Moreover, we apply the definitions $pK = -\log_{10}(K)$, $pL = -\log_{10}(L)$, and the ratio $R = P^0/P^+$.

The lines in Fig. 1 A represent fits of Eq. 1 with the parameters reported in the legends. Eq. 1 describes well the sigmoidal pH dependence of WT CIC-K1 and CIC-Ka (Fig. 1 A), with $pK = 8.7$, $pL = 11.8$, and $R = 0.07$ for CLC-K1, i.e., deprotonation of K165 is predicted to reduce the open probability to a value of 7% compared to the protonated state. For the unmodified K165C and the mutant modified by MTSEH and MTSET, no biphasic pH dependence is visible and the data can be well described by a simple blocking deprotonation process:

$$P = \frac{1}{\left(1 + \frac{L}{[\text{H}]}\right)} \quad (2)$$

(Figs. 5 B, 7 C, and 8 B), with pL ranging from 10.8 to 11.1, similar to the value found for WT CIC-K. The most interesting case regards the pH dependence of MTSEA-modified K165C. The biphasic pH dependence is very well described by Eq. 1, with $pK = 7.6$, $pL = 11.1$, and $R = 0.37$ (Fig. 6 C). Again pL is similar to the other cases, whereas pK is about one pH unit more acidic than for WT CIC-K1. Most notably, R is significantly larger than for WT, suggesting that deprotonation of the MTSEA moiety has only a relatively small effect on the open probability.

CONCLUSIONS

The kidney plays a pivotal role in pH regulation. In particular, the thick ascending limb of Henle's loop, where CIC-Kb is expressed, effectively participates in the maintenance of the acid-base balance (56). Thus the pH dependence of CLC-K channels is probably of physiological relevance and represents an interesting topic of study. Here, we reveal that CLC-K channels are inhibited at alkaline pH, resulting in an overall biphasic pH dependence with a block of the currents both at extremely acidic and at alkaline pH values. A similar behavior was found in the CIC-2 channel (34,37,39,43,44). Inhibition by acidic pH results from the

protonation of a homologous histidine in both channels (25,43). In contrast, a different mechanism underlies the inhibition of these channels by alkaline pH. CIC-2 is modulated via deprotonation of the gating glutamate (39,43,44). However, as this residue is a valine in CLC-K channels, other mechanisms must underlie the block of CLC-K currents at alkaline pH.

To determine whether low $[H^+]_{ext}$ affects the ion permeation of the channel or acts on the open probability, we estimated the conductance of WT CIC-K1 at pH 7.3 and 10 by noise analysis. At pH 10, the single-channel conductance was only slightly smaller, showing that the alkaline block mainly depends on an allosteric decrease of the open probability. Even if the reduction of conductance is not responsible for alkaline block, it is significant. Thus, we might speculate that deprotonation of K165 could weakly affect Cl^- permeation across the channel. However, it has to be kept in mind that the noise analysis is complicated by the fact that CLC proteins have two pores, each with a proper gate and an additional common gate. Therefore, a consistent apparent variability of the single-channel current (maximally by a factor of 2) can be caused indirectly by effects on the relative contributions of single/double pore openings to the noise, thus reflecting a gating rather than a conductance effect. Further investigation is required to resolve this question.

Using the homology model of CIC-Ka (26), we identified a pore lysine K165 that is involved in the modulation of the channel by alkaline pH. Lysine 165 is highly conserved in CLC proteins (50,53) and positioned next to valine 166, which corresponds to the conserved gating glutamate in CLC-Ks. Based on our extensive analysis of the pH dependence of point mutants of K165 and the cysteine-modified K165C variants in the background of CIC-K1, we can conclude that deprotonation of K165, with a pK of ~ 8.7 , leads to dramatic inhibition of CLC-K channels. It is interesting that the apparent pK of K165 is closer to the physiological pH range than that of free lysine (pK ~ 10.5), suggesting that the ability of K165 to inactivate CLC-Ks in alkaline conditions could have a physiological relevance.

Furthermore, modification of K165C with nontitratable MTS reagents uncovered an additional pH-dependent inhibitory process occurring at more alkaline pH values ($pH \geq 11$). In the absence of an investigation at pH values > 11 , we can only speculate about the causes of this further process. Plausible hypotheses are that this block could be due to deprotonation of an unknown residue or to a direct block of the pore by OH^- ions. Finally, our results demonstrate that a positive charge at position 165 is not the only determinant of the open probability, but that the general chemical and sterical properties of the residue are equally important. In fact, modification of K165C by the uncharged and nontitratable MTSEH leads to an increase in currents similar to that observed with modification by MTSEA, whereas modification by the positive MTSET does not in-

crease the current amplitude. Previous studies have demonstrated the involvement of K165 in mechanisms of gating of CLC proteins. The mutation to alanine of the homologous residue in CIC-1, K231, completely modifies the channel kinetics. In fact at hyperpolarizing potentials, K231A shows activating currents instead of the peculiar deactivating kinetics observed in the WT (54). The mutant K165R of CIC-0 exhibits inwardly rectifying currents, which demonstrates that the conservative mutation of lysine to arginine at position 165 is enough to modify deeply the gating of CIC-0 (57). The less conservative mutant, K165C, in CIC-0 lacks functional expression. However, it can be activated by MTSEA modification (55). Taking advantage of this, Lin and Chen (55) constructed homodimers and heterodimers of this mutant and applied MTSEA modification to these to understand how this residue is involved in the gating of CIC-0 (55). They concluded that the mutation of K165 affects both slow and fast gating of the channel (55). An interesting finding in their study was that single-channel recordings of unmodified K165C-K165 heterodimers in the background of the C212S mutant of CIC-0 (55) displayed openings of a single pore (presumably the K165 protopore). Since by definition the slow gate acts on both pores simultaneously, this observation by Chen and colleagues suggests that the drastic reduction of the open probability of the K165C pore reflects an effect on the fast gate, and that the slow gate is only indirectly affected. Matters are more complex for CLC-K channels, because in these channels, the gating glutamate is substituted by a valine (V166), and little is known about the mechanisms of CLC-K channel gating. In fact, the alkaline pH effect might provide a tool to gain more insight into these mechanisms. Nevertheless, this residue is important for the gating of both CLC channels bearing the gating glutamate (CIC-0) and those lacking it (CLC-Ks). It will be interesting to find out the details of the gating processes influenced by K165 in CLC-K channels. Finally, another study (58) highlighted that the homologous lysine in CIC-5 (K210) can be substituted by many different residues without gross impairment of function, suggesting, however, that K210 plays a role in the determination of the anionic specificity of this transporter and stressing that this residue plays different roles in different CLC proteins.

Our results also indicate that deprotonation of K165 in WT CIC-K1 does not completely shut the channel. From our quantitative model, we obtained a residual open probability of 7% of the value for the protonated lysine. The model also nicely described the pH dependence of the MTSEA-modified K165C mutant, for which the open probability of the protonated and deprotonated forms is predicted to differ by less than a factor of 3.

In summary, we identify here the residue responsible for alkaline block close to the physiological pH range. In addition, we reveal that this residue is involved in the gating of CLC-K channels. This information is quite

surprising: CLC-Ks lack the gating glutamate, but the same region of the protein determines their gating machinery.

SUPPORTING MATERIAL

Five figures are available at [http://www.biophysj.org/biophysj/supplemental/S0006-3495\(13\)00631-0](http://www.biophysj.org/biophysj/supplemental/S0006-3495(13)00631-0).

This work was supported by Telethon Italy (grant GGP12008), the Italian Ministry of Education (progetto PRIN), and the Compagnia San Paolo.

We thank T. J. Jentsch for all wild-type clones and F. Quartino, A. Barbin, and D. Magliozzi for technical assistance.

REFERENCES

- Kieferle, S., P. Fong, ..., T. J. Jentsch. 1994. Two highly homologous members of the CIC chloride channel family in both rat and human kidney. *Proc. Natl. Acad. Sci. USA*. 91:6943–6947.
- Uchida, S., S. Sasaki, ..., F. Marumo. 1993. Molecular cloning of a chloride channel that is regulated by dehydration and expressed predominantly in kidney medulla. *J. Biol. Chem.* 268:3821–3824.
- Jentsch, T. J., T. Maritzen, and A. A. Zdebik. 2005. Chloride channel diseases resulting from impaired transepithelial transport or vesicular function. *J. Clin. Invest.* 115:2039–2046.
- Jentsch, T. J., I. Neagoe, and O. Scheel. 2005. CLC chloride channels and transporters. *Curr. Opin. Neurobiol.* 15:319–325.
- Estévez, R., T. Boettger, ..., T. J. Jentsch. 2001. Barttin is a Cl⁻ channel β -subunit crucial for renal Cl⁻ reabsorption and inner ear K⁺ secretion. *Nature*. 414:558–561.
- Rickheit, G., H. Maier, ..., T. J. Jentsch. 2008. Endocochlear potential depends on Cl⁻ channels: mechanism underlying deafness in Bartter syndrome IV. *EMBO J.* 27:2907–2917.
- Zdebik, A. A., P. Wangemann, and T. J. Jentsch. 2009. Potassium ion movement in the inner ear: insights from genetic disease and mouse models. *Physiology (Bethesda)*. 24:307–316.
- Birkenhäger, R., E. Otto, ..., F. Hildebrandt. 2001. Mutation of BSND causes Bartter syndrome with sensorineural deafness and kidney failure. *Nat. Genet.* 29:310–314.
- Fischer, M., A. G. Janssen, and C. Fahlke. 2010. Barttin activates CIC-K channel function by modulating gating. *J. Am. Soc. Nephrol.* 21:1281–1289.
- Scholl, U., S. Hebeisen, ..., C. Fahlke. 2006. Barttin modulates trafficking and function of CIC-K channels. *Proc. Natl. Acad. Sci. USA*. 103:11411–11416.
- Simon, D. B., R. S. Bindra, ..., R. P. Lifton. 1997. Mutations in the chloride channel gene, CLCNKB, cause Bartter's syndrome type III. *Nat. Genet.* 17:171–178.
- Simon, D. B., F. E. Karet, ..., R. P. Lifton. 1996. Bartter's syndrome, hypokalaemic alkalosis with hypercalciuria, is caused by mutations in the Na-K-2Cl cotransporter NKCC2. *Nat. Genet.* 13:183–188.
- Simon, D. B., F. E. Karet, ..., R. P. Lifton. 1996. Genetic heterogeneity of Bartter's syndrome revealed by mutations in the K⁺ channel, ROMK. *Nat. Genet.* 14:152–156.
- Schlingmann, K. P., M. Konrad, ..., S. Waldegger. 2004. Salt wasting and deafness resulting from mutations in two chloride channels. *N. Engl. J. Med.* 350:1314–1319.
- Liantonio, A., A. Accardi, ..., M. Pusch. 2002. Molecular requisites for drug binding to muscle CLC-1 and renal CLC-K channel revealed by the use of phenoxy-alkyl derivatives of 2-(p-chlorophenoxy)propionic acid. *Mol. Pharmacol.* 62:265–271.
- Liantonio, A., A. Picollo, ..., D. C. Camerino. 2006. Activation and inhibition of kidney CLC-K chloride channels by fenamates. *Mol. Pharmacol.* 69:165–173.
- Liantonio, A., A. Picollo, ..., D. C. Camerino. 2008. Molecular switch for CLC-K Cl⁻ channel block/activation: optimal pharmacophoric requirements towards high-affinity ligands. *Proc. Natl. Acad. Sci. USA*. 105:1369–1373.
- Liantonio, A., M. Pusch, ..., D. Conte Camerino. 2004. Investigations of pharmacologic properties of the renal CLC-K1 chloride channel co-expressed with barttin by the use of 2-(p-chlorophenoxy)propionic acid derivatives and other structurally unrelated chloride channel blockers. *J. Am. Soc. Nephrol.* 15:13–20.
- Picollo, A., A. Liantonio, ..., M. Pusch. 2007. Mechanism of interaction of niflumic acid with heterologously expressed kidney CLC-K chloride channels. *J. Membr. Biol.* 216:73–82.
- Picollo, A., A. Liantonio, ..., M. Pusch. 2004. Molecular determinants of differential pore blocking of kidney CLC-K chloride channels. *EMBO Rep.* 5:584–589.
- Zifarelli, G., A. Liantonio, ..., M. Pusch. 2010. Identification of sites responsible for the potentiating effect of niflumic acid on CIC-Ka kidney chloride channels. *Br. J. Pharmacol.* 160:1652–1661.
- Gradogna, A., and M. Pusch. 2010. Molecular pharmacology of kidney and inner ear CLC-K chloride channels. *Front. Pharmacol.* 1:130.
- Uchida, S., S. Sasaki, ..., F. Marumo. 1995. Localization and functional characterization of rat kidney-specific chloride channel, CIC-K1. *J. Clin. Invest.* 95:104–113.
- Waldegger, S., N. Jeck, ..., H. W. Seyberth. 2002. Barttin increases surface expression and changes current properties of CIC-K channels. *Pflügers Arch.* 444:411–418.
- Gradogna, A., E. Babini, ..., M. Pusch. 2010. A regulatory calcium-binding site at the subunit interface of CLC-K kidney chloride channels. *J. Gen. Physiol.* 136:311–323.
- Gradogna, A., C. Fenollar-Ferrer, ..., M. Pusch. 2012. Dissecting a regulatory calcium-binding site of CLC-K kidney chloride channels. *J. Gen. Physiol.* 140:681–696.
- Iyer, R., T. M. Iverson, ..., C. Miller. 2002. A biological role for prokaryotic CIC chloride channels. *Nature*. 419:715–718.
- Accardi, A., and C. Miller. 2004. Secondary active transport mediated by a prokaryotic homologue of CIC Cl⁻ channels. *Nature*. 427:803–807.
- Friedrich, T., T. Breiderhoff, and T. J. Jentsch. 1999. Mutational analysis demonstrates that CIC-4 and CIC-5 directly mediate plasma membrane currents. *J. Biol. Chem.* 274:896–902.
- Picollo, A., and M. Pusch. 2005. Chloride/proton antiporter activity of mammalian CLC proteins CIC-4 and CIC-5. *Nature*. 436:420–423.
- Zifarelli, G., and M. Pusch. 2009. Conversion of the 2 Cl⁻/1 H⁺ antiporter CIC-5 in a NO₃⁻/H⁺ antiporter by a single point mutation. *EMBO J.* 28:175–182.
- Hanke, W., and C. Miller. 1983. Single chloride channels from *Torpedo* electroplax. Activation by protons. *J. Gen. Physiol.* 82:25–45.
- Rychkov, G. Y., M. Pusch, ..., A. H. Bretag. 1996. Concentration and pH dependence of skeletal muscle chloride channel CIC-1. *J. Physiol.* 497:423–435.
- Jordt, S. E., and T. J. Jentsch. 1997. Molecular dissection of gating in the CIC-2 chloride channel. *EMBO J.* 16:1582–1592.
- Saviane, C., F. Conti, and M. Pusch. 1999. The muscle chloride channel CIC-1 has a double-barreled appearance that is differentially affected in dominant and recessive myotonia. *J. Gen. Physiol.* 113:457–468.
- Chen, M. F., and T. Y. Chen. 2001. Different fast-gate regulation by external Cl⁻ and H⁺ of the muscle-type CIC chloride channels. *J. Gen. Physiol.* 118:23–32.
- Arreola, J., T. Begenisich, and J. E. Melvin. 2002. Conformation-dependent regulation of inward rectifier chloride channel gating by extracellular protons. *J. Physiol.* 541:103–112.
- Dutzler, R., E. B. Campbell, and R. MacKinnon. 2003. Gating the selectivity filter in CIC chloride channels. *Science*. 300:108–112.

39. Niemeyer, M. I., L. P. Cid, ..., F. V. Sepúlveda. 2003. A conserved pore-lining glutamate as a voltage- and chloride-dependent gate in the ClC-2 chloride channel. *J. Physiol.* 553:873–879.
40. Traverso, S., G. Zifarelli, ..., M. Pusch. 2006. Proton sensing of CLC-0 mutant E166D. *J. Gen. Physiol.* 127:51–65.
41. Zifarelli, G., A. R. Murgia, ..., M. Pusch. 2008. Intracellular proton regulation of ClC-0. *J. Gen. Physiol.* 132:185–198.
42. Zifarelli, G., and M. Pusch. 2010. The role of protons in fast and slow gating of the *Torpedo* chloride channel ClC-0. *Eur. Biophys. J.* 39:869–875.
43. Niemeyer, M. I., L. P. Cid, ..., F. V. Sepúlveda. 2009. Voltage-dependent and -independent titration of specific residues accounts for complex gating of a ClC chloride channel by extracellular protons. *J. Physiol.* 587:1387–1400.
44. Sánchez-Rodríguez, J. E., J. A. De Santiago-Castillo, ..., J. Arreola. 2012. Sequential interaction of chloride and proton ions with the fast gate steer the voltage-dependent gating in ClC-2 chloride channels. *J. Physiol.* 590:4239–4253.
45. Bennetts, B., M. W. Parker, and B. A. Cromer. 2007. Inhibition of skeletal muscle ClC-1 chloride channels by low intracellular pH and ATP. *J. Biol. Chem.* 282:32780–32791.
46. Waldegger, S., and T. J. Jentsch. 2000. Functional and structural analysis of ClC-K chloride channels involved in renal disease. *J. Biol. Chem.* 275:24527–24533.
47. Accardi, A., and M. Pusch. 2003. Conformational changes in the pore of CLC-0. *J. Gen. Physiol.* 122:277–293.
48. Heinemann, S. H., and F. Conti. 1992. Nonstationary noise analysis and application to patch-clamp recordings. *Methods Enzymol.* 207:131–148.
49. Pusch, M., K. Steinmeyer, and T. J. Jentsch. 1994. Low single channel conductance of the major skeletal muscle chloride channel, ClC-1. *Biophys. J.* 66:149–152.
50. Dutzler, R., E. B. Campbell, ..., R. MacKinnon. 2002. X-ray structure of a ClC chloride channel at 3.0 Å reveals the molecular basis of anion selectivity. *Nature.* 415:287–294.
51. Lin, C. W., and T. Y. Chen. 2003. Probing the pore of ClC-0 by substituted cysteine accessibility method using methane thiosulfonate reagents. *J. Gen. Physiol.* 122:147–159.
52. Accardi, A., S. Lobet, ..., R. Dutzler. 2006. Synergism between halide binding and proton transport in a ClC-type exchanger. *J. Mol. Biol.* 362:691–699.
53. Mindell, J. A., and M. Maduke. 2001. ClC chloride channels. *Genome Biol.* 2:S3003.
54. Fahlke, C., H. T. Yu, ..., A. L. George, Jr. 1997. Pore-forming segments in voltage-gated chloride channels. *Nature.* 390:529–532.
55. Lin, C. W., and T. Y. Chen. 2000. Cysteine modification of a putative pore residue in ClC-0: implication for the pore stoichiometry of ClC chloride channels. *J. Gen. Physiol.* 116:535–546.
56. Koeppen, B. M. 2009. The kidney and acid-base regulation. *Adv. Physiol. Educ.* 33:275–281.
57. Ludewig, U., T. J. Jentsch, and M. Pusch. 1997. Inward rectification in ClC-0 chloride channels caused by mutations in several protein regions. *J. Gen. Physiol.* 110:165–171.
58. De Stefano, S., M. Pusch, and G. Zifarelli. 2011. Extracellular determinants of anion discrimination of the Cl⁻/H⁺ antiporter protein ClC-5. *J. Biol. Chem.* 286:44134–44144.

Supporting Material

Alkaline pH block of CLC-K kidney chloride channels mediated by a pore lysine residue.

Antonella Gradogna¹, Michael Pusch¹

¹ Istituto di Biofisica, CNR, Via De Marini 6, 16149 Genoa, Italy.

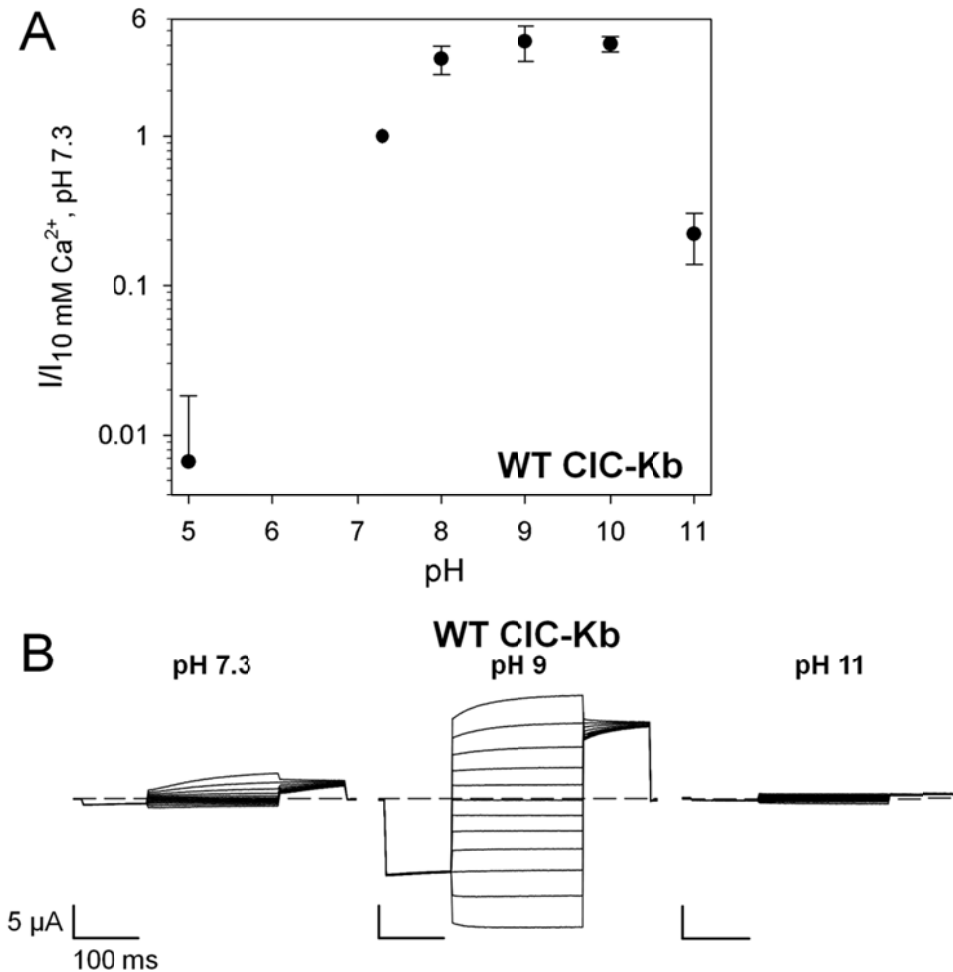


FIGURE S1. Effect of alkaline pH on WT CIC-Kb. CIC-Kb is inhibited by alkaline pH with currents at pH 11 that are ~ 22% of the currents at pH 7.3, but only 5% of the maximum level of current recorded at pH 9. (A) Mean currents of CIC-Kb at 60 mV as a function of pH, normalized to the current at pH 7.3 (n = 4, except pH 5 for which n = 3). Error bars indicate SD. (B) Typical current traces of WT CIC-Kb in response to the “IV pulse” protocol at pH 7.3, 9, and 11.

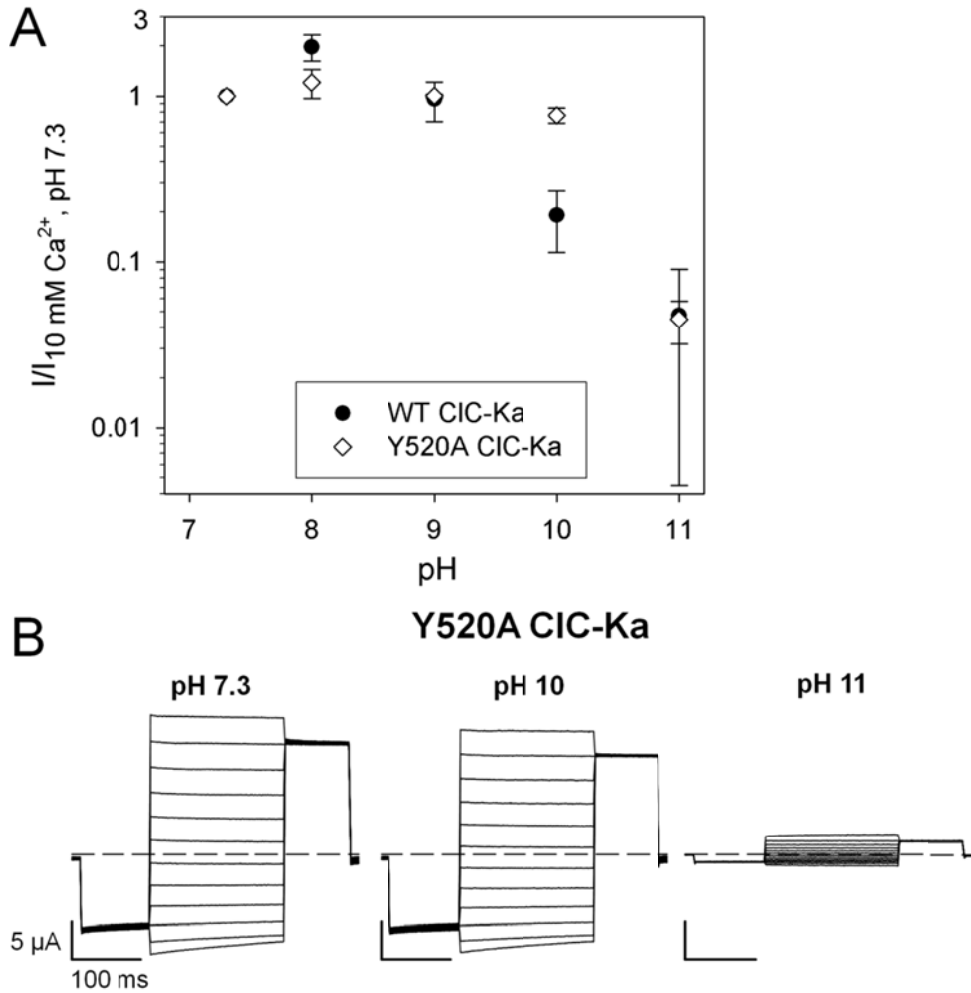


FIGURE S2. Y520A CIC-Ka currents are affected only by extreme alkaline pH. (A) Mean currents of WT CIC-Ka ($n \geq 11$; filled circles) and Y520A CIC-Ka ($n \geq 4$; empty rhombi) recorded at 60 mV were normalized to current at pH 7.3 and plotted versus pH values. Data for WT CIC-Ka are the same as in Fig. 1A. Error bars indicate SD. (B) Representative current traces for Y520A CIC-Ka in response to the “IV pulse” protocol at different pH values.

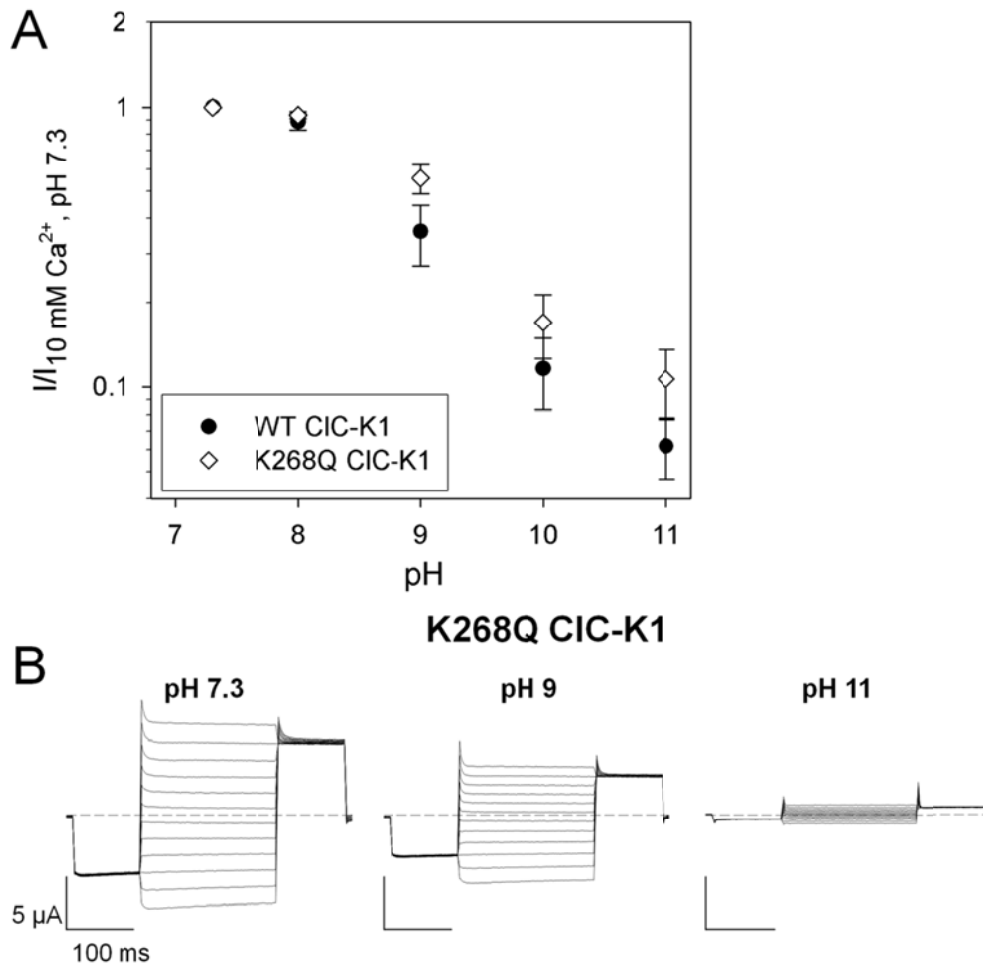


FIGURE S3. K268Q CIC-K1 currents are affected by alkaline pH similarly to WT. (A) Mean currents of WT CIC-K1 ($n = 10$; filled circles) and K268Q CIC-K1 ($n = 3$; empty rhombi) recorded at 60 mV were normalized to current at pH 7.3 and plotted versus pH values. Error bars indicate SD. Data for WT CIC-K1 are the same as in Fig. 1A, Fig. 5B, Fig. 6C, Fig. 7C, and Fig. 8B. (B) Current traces of K268Q CIC-K1 in response to the “IV pulse” protocol at different pH values.

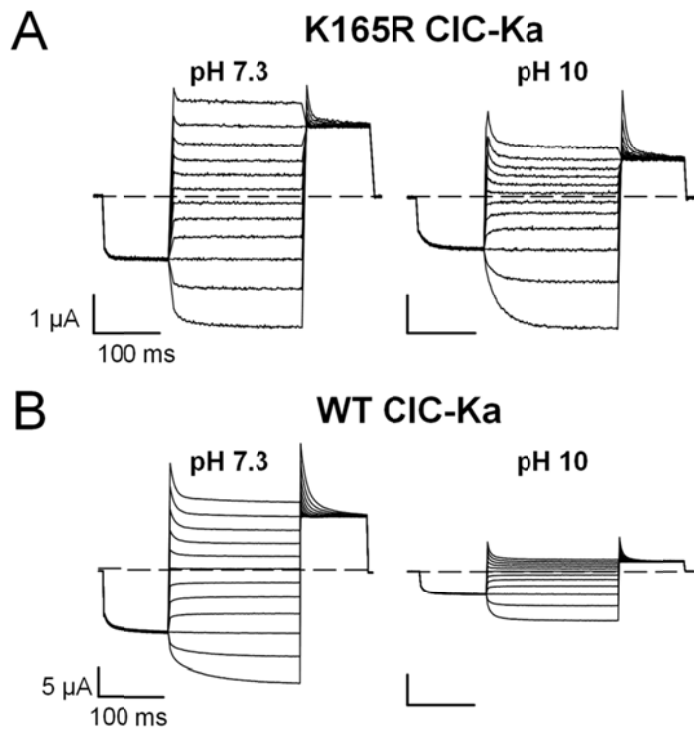


FIGURE S4. The mutant K165R CIC-Ka is less affected by alkaline pH than WT. At all pH tested this mutant shows a minor response to alkaline pH, for example at pH 10 the K165R currents are ~ 50% of the currents in control conditions, while the currents of WT CIC-Ka are only ~ 19% of the current at 7.3. Voltage clamp traces of oocytes expressing K165R CIC-Ka (A) and WT CIC-Ka (B) in response to the “IV pulse” protocol (see Materials and Methods) at pH 7.3 and 10.

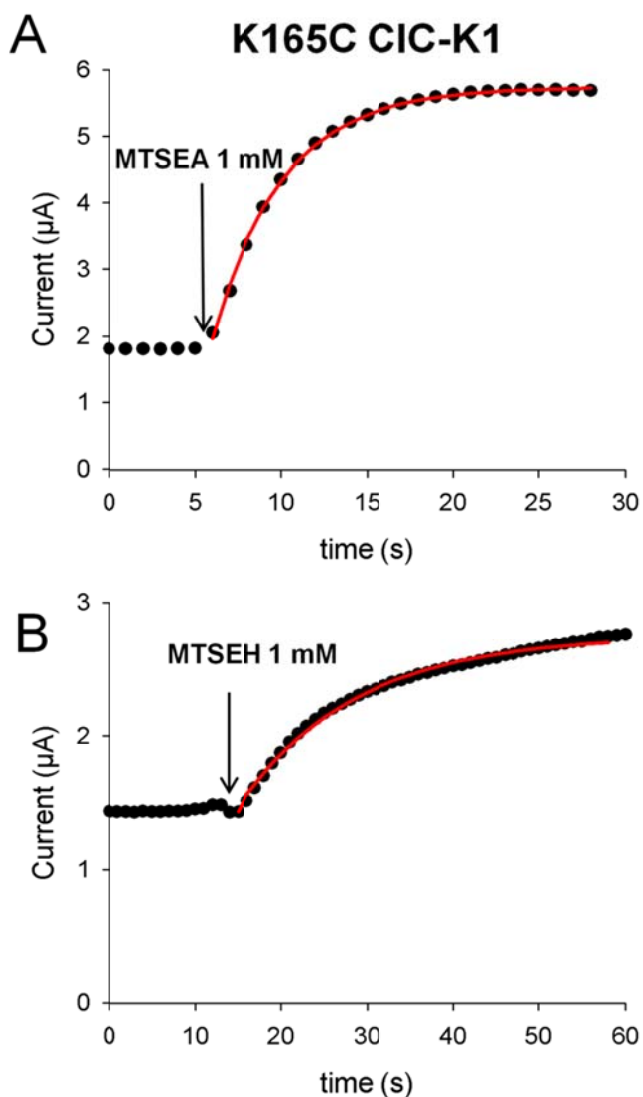


FIGURE S5. Modification by MTS reagents of K165C CIC-K1. The channels were stimulated with repetitive pulse to 60 mV and 1 mM MTS reagent was continuously applied. The current response of the mutant was plotted as function of time. Red lines represent exponential fits. (A) For MTSEA time constant $\tau = (4.9 \pm 1.0)$ s and reaction rate $k = (206 \pm 40)$ $\text{s}^{-1} \text{M}^{-1}$ came from $n = 5$ experiments. (B) For MTSEH $\tau = (8.9 \text{ s} \pm 1.8)$ s, $k = (112 \pm 23)$ $\text{s}^{-1} \text{M}^{-1}$ were estimated by $n = 3$ experiments. All errors are SD.